

Patterning Fluorescent Quantum Dot Nanocomposites by Reactive Inkjet Printing

Bin Bao, Mingzhu Li, Yuan Li, Jieke Jiang, Zhenkun Gu, Xingye Zhang, Lei Jiang, and Yanlin Song*

Semiconductor quantum dots (QDs) are a class of nanomaterials, which exhibit exceptional optoelectronic properties because of their size-dependent quantum confinement effects.^[1] Accordingly, QDs have enormous potentials as an essential component in high-efficiency luminescent devices,^[2] light-emitting devices,^[3] photovoltaic cells,^[4] and other related devices. To integrate them with the abovementioned solid-state devices, the QDs must be precisely and accurately patterned in predetermined locations on a substrate.^[5] Presently, there are two main strategies to pattern nanomaterials: the *ex situ* and *in situ* approaches. For *ex situ* approach, nanomaterials are firstly synthesized hydrothermally or solvothermally and then patterned,^[6] which suffers from drawbacks such as tedious synthesis procedures and tiresome purification processes. Whereas the *in situ* approach is able to carry out functional material synthesizing by pre patterning their precursors, which is fast and cost effective, providing a possible way for large-area patterning.^[7] For example, Duan and coworkers incorporated a divalent cadmium ion-contained precursor into the photopolymerizable resins and fabricated 3D luminescent microstructures by combining multiphoton polymerization and *in situ* synthesis of CdS nanoparticles.^[8] Chen and co-workers utilized a microfluidic spinning technique to fabricate multidimensional microreactors for

the synthesis of fluorescent CdS and ZnS nanocrystals.^[9] Recently, a more straightforward method to *in situ* fabricate nanoparticles has been proposed by Chiolerio et al.^[10] In this method, silver nitrate solution was directly inkjet-printed onto mesoporous silicon substrates and subsequently reduced into silver nanoparticles by the hydride-covered silicon surface.^[10a] The as-fabricated silver nanoparticles hugely enhanced the Raman signals, which was promising to construct sensing platforms.^[10b]

So far, a variety of techniques have been applied to pattern functional nanomaterials, such as mask-based lithography,^[11] microcontact printing,^[12] nanoimprint lithography,^[13] and inkjet printing.^[14] Among these patterning technologies, inkjet printing is particularly attractive because of its direct-writing, mask-free, and flexible characteristics of the substrate. As a versatile inkjet printing technique, reactive inkjet printing has caught much attention to fabricate patterns in a more cost-effective way, which combines the processes of material deposition and reaction.^[15] Moreover, the wide spectrum of the reactive inks allows one to fabricate various patterns that perform different functionalities.^[16–18]

Recently, nanocomposites that comprise a polymer host doped with semiconductor nanoparticles have been widely exploited because they combine the advantages of each component and their properties are easily tailored by combining different constituents.^[19] For example, semiconductor-polymer nanocomposites reserve fluorescent property of the semiconductor and admirable processing property of the polymer.^[20] Semiconductor-photonic crystal (PC) nanocomposites can emit modified fluorescence through the modulation of the photonic bandgap.^[21] The photoinitiator-free UV-cured semiconductor magnetite-polymer nanocomposites can be used in magnetic filter devices.^[22] The UV-curable titanium oxide/silver-polymer nanocomposites show outstanding piezoresistive properties, which can be used in strain measurement.^[23] The wide range of available inks makes the reactive inkjet printing an efficient technique to fabricate the above mentioned nanocomposite patterns. However, it is still a challenge to *in situ* fabricate QD-contained nanocomposites by reactive inkjet printing because of the difficulty in formulating the reactive inks. Herein, we fabricate fluorescent CdS QD-polymer nanocomposite patterns through inkjet printing a cadmium source-loaded ink, followed by treating the patterns with hydrogen sulfide gas. Furthermore, CdS QD-PC nanocomposites with enhanced fluorescence are fabricated by introducing

Dr. B. Bao, Dr. M. Li, Y. Li, J. Jiang, Z. Gu, Dr. X. Zhang,
Prof. L. Jiang, Prof. Y. Song
Beijing National Laboratory for Molecular Sciences
Zhongguancun North First Street
Beijing 100190,
P.R. China
E-mail: ylsong@iccas.ac.cn



Dr. B. Bao, Dr. M. Li, Y. Li, J. Jiang, Z. Gu, Dr. X. Zhang,
Prof. L. Jiang, Prof. Y. Song
Key Laboratory of Green Printing
Institute of Chemistry, Chinese Academy of Sciences
Beijing 100190, P.R. China

Dr. B. Bao, Dr. M. Li, Y. Li, J. Jiang, Z. Gu, Dr. X. Zhang, Prof. L. Jiang,
Prof. Y. Song

Key Laboratory of Organic Solids
Institute of Chemistry, Chinese Academy of Sciences
Beijing 100190, P.R. China

Dr. B. Bao, Y. Li, J. Jiang, Z. Gu
School of Chemistry and Chemical Engineering
University of Chinese Academy of Sciences
Beijing 100049, P.R. China

DOI: 10.1002/sml.201403005

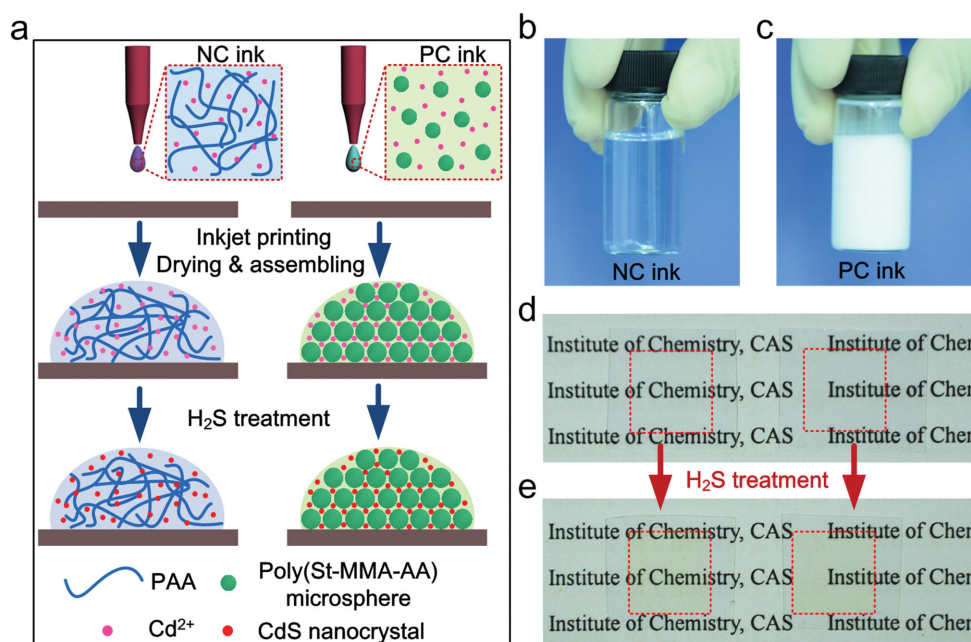


Figure 1. Fluorescent CdS QD-polymer and CdS QD-PC nanocomposites are patterned by reactive inkjet printing. a) Schematic illustrations of the nanocomposite fabricating processes. NC or PC inks are inkjet-printed, followed by solution evaporating or poly(St–MMA–AA) microsphere assembling in the ink. The patterns are subsequently treated by hydrogen sulfide gas to in situ fabricate CdS QD-polymer or CdS QD-PC nanocomposites. b, c) Photographs of the NC ink solution and the PC ink suspension which are loaded with divalent cadmium ions, respectively. d, e) Photographs of 1 cm × 1 cm patterns printed on PDMS surfaces before and after H₂S treatment, respectively. The as-printed patterns are transparent and become yellowish after H₂S treatment. The left panel is printed with the NC ink and the right panel is printed with the PC ink, respectively.

monodispersed poly(styrene–methyl methacrylate–acrylic acid) (poly(St–MMA–AA)) microspheres that serve as the PC building blocks into the inks. The fabricating process is straightforward and flexible, which would find diverse applications in patterning nanocomposites for optoelectronic devices.

Figure 1 shows that fluorescent CdS QD-polymer and CdS QD-PC nanocomposite patterns are fabricated by reactive inkjet printing. The fabricating processes are schematically illustrated in Figure 1a. For the fabrication of CdS QD-polymer nanocomposites, poly acrylic acid (PAA) was selected as the polymer matrix because of its high water solubility and excellent printability. Meanwhile, highly monodispersed poly(St–MMA–AA) microsphere latex loaded with divalent cadmium ions was formulated as the ink for the preparation of CdS QD-PC nanocomposites. The two cadmium source-loaded inks were inkjet-printed, followed by solution evaporation and poly(St–MMA–AA) microsphere assembly. Subsequently, CdS QD-PAA and CdS QD-PC nanocomposites were in situ generated by treating the printed patterns with hydrogen sulfide gas. PAA ink solution loaded with cadmium ions (called as NC ink) was transparent (Figure 1b), with surface tension measured as $33.36 \pm 0.11 \times 10^{-3} \text{ N m}^{-1}$, and viscosity as $10.21 \pm 1.39 \text{ mPa S}$. For the milky cadmium ion-loaded poly(St–MMA–AA) microsphere ink suspension (called as PC ink, Figure 1c), the surface tension was measured as $42.82 \pm 0.26 \times 10^{-3} \text{ N m}^{-1}$, and the viscosity was $29.37 \pm 2.15 \text{ mPa S}$. Both the surface tension and the viscosity were important for the printability. These inks could be steady and consecutively ejected from the printing nozzle, and the morphology of the deposited ink

droplets could be well controlled to avoid the coffee ring effect.^[24] Patterns constructed by dot arrays were printed on hydrophobic polydimethylsiloxane (PDMS) substrates, as shown in Figure 1d,e. The as-printed patterns were transparent and became yellowish after hydrogen sulfide gas treatment, indicating the production of CdS.

Firstly, the fabrication of CdS QD-PAA nanocomposite patterns were investigated, as shown in **Figure 2**. Optical microscope photograph of the CdS QD-PAA nanocomposite dot arrays are shown in Figure 2a, demonstrating their great size homogeneity. The PDMS substrate was hydrophobic, with contact angle of $123.2 \pm 3.0^\circ$, as shown by the insert image in Figure 2a. The hydrophobicity of the substrate resulted in depinning of the three phase contact line of the ink droplets during their solution evaporation; hence, prevented the formation of coffee ring, leading to dome-shaped dot patterns.^[24a,25] The dome-shaped patterns were confirmed by scanning electron microscope (SEM) observation (Figure 2b). For comparison, the same ink was printed onto hydrophilic polyethylene terephthalate (PET) surface with water contact angle of $67.4^\circ \pm 1.8^\circ$ (Figure S1, Supporting Information). The hydrophilicity of the substrate would lead to the pinning of the three phase contact line of the ink droplets, hence coffee-ring-shaped patterns were formed after solvent evaporation (Figure S1b, Supporting Information).^[26] In most device applications, coffee ring effect would result in inhomogeneity of the printed features; hence failure of the devices, thus needing to be avoided.^[27] In this contribution, to fabricate patterns with homogeneous fluorescence, PDMS was selected as a substrate to eliminate the coffee ring effect.

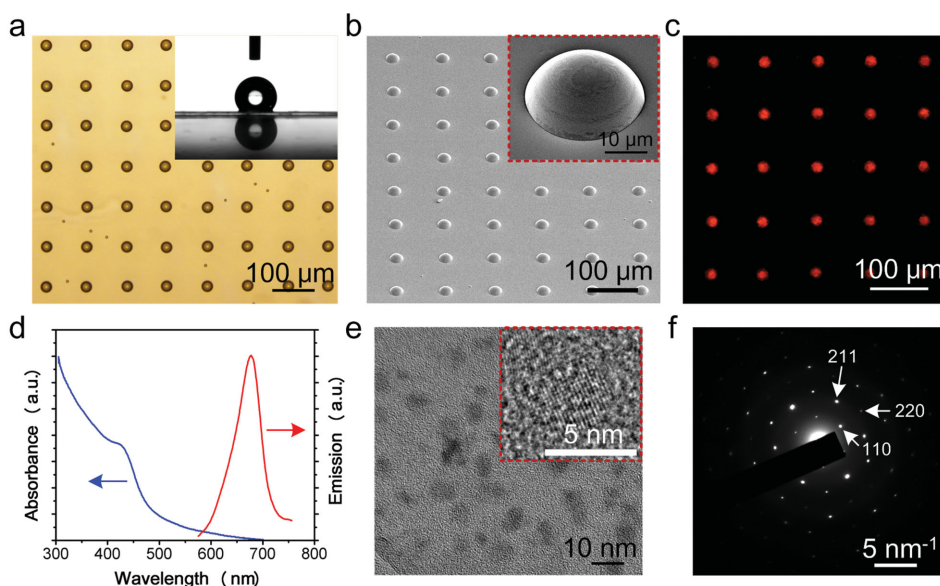


Figure 2. Fluorescent CdS QD-PAA nanocomposite patterns are in situ fabricated by reactive inkjet printing. a) Optical microscope photograph of the CdS QD-PAA nanocomposite dome array patterns, demonstrating their high homogeneity. Insert is the contact angle of the PDMS substrate, indicating its hydrophobicity which could prevent the coffee ring effect. b) 45° SEM observation of the CdS QD-PAA nanocomposite patterns. Insert is a magnified image of a single dome. c) Fluorescent image of the dome array. d) Absorbance and emission spectra of the CdS QD-PAA nanocomposites. e) TEM observation of the CdS QD-PAA nanocomposites. Insert is a high resolution TEM image of a single CdS nanocrystal. f) SAED pattern of CdS nanocrystals, indicating their face-centered cubic structure.

The optical properties and morphological structures of the as-fabricated CdS QD-PAA nanocomposites were investigated as shown in Figure 2c–f. Fluorescence microscope image displayed that orange red fluorescence was emitted by the printed patterns (Figure 1c). The ultraviolet-visible (UV–vis) absorbance and fluorescence emission spectra revealed that the CdS QD-PAA nanocomposites had an absorbance at about 415 nm and a narrow emission peak at 678 nm, respectively. From the absorption onset of the nanocomposites, the average size of the CdS QDs could be calculated by using Brus Equation,^[28] which is expressed as

$$\Delta E(r) = E_{\text{gap}} + \frac{h^2}{8r^2} \left(\frac{1}{m_e^*} + \frac{1}{m_h^*} \right) \quad (1)$$

where $\Delta E(r)$ was the bandgap energy of the CdS QDs, E_{gap} was the bandgap energy of bulk CdS (2.42 eV), h was the Planck's constant, r was the average size of the nanoparticles, m_e^* was the effective mass of electron (0.19 m_e in CdS), and m_h^* was the effective mass of hole (0.8 m_e in CdS). The calculated average particle size of the CdS QDs was 10.4 nm. To confirm the estimated particle sizes of the CdS QDs, transmission electron microscope (TEM) observation of the nanocomposites was carried out, as shown in Figure 2e. The measured diameter was 7.1 ± 1.6 nm, which was smaller than the calculated values. This mismatch between the calculated and measured values was possibly attributed to the red shift of the tested UV–vis absorbance of the sample. It was noteworthy that the particle size was larger than Duan's results.^[8] This was mostly because that the space available within the linear PAA polymer matrix was larger than that in the crosslinking polymer networks, hence the size of the in situ synthesized CdS QDs was less confined during the

gas treatment process. The high resolution TEM image of a single CdS nanocrystal inserted in Figure 2e clearly revealed the lattice fringes, which evidenced the formation of crystalline CdS QDs. Furthermore, selected area electron diffraction (SAED) pattern in Figure 2f indicated that the crystalline CdS QDs had a face-centered cubic structure.^[8]

Photonic crystals that were constructed by periodic dielectric materials were widely used to modify spontaneous emission because of their special light manipulation properties.^[29] Previously, fluorescent contrast was amplified by applying PCs to the photochromic optical storage system.^[30] Fluorescent signals were enhanced by PCs to perform high sensitive chemical detections.^[31] Moreover, fluorescence molecule-doped PC domes were inkjet-printed to fabricate wide viewing-angle displays.^[24a] In this work, monodispersed poly(St–MMA–AA) microspheres that served as the PC building blocks coupled with divalent cadmium source were introduced into the inks to in situ fabricate CdS QD-PC nanocomposite patterns with enhanced fluorescence. One major challenge to fabricate PC domes by inkjet printing was to achieve assembly of the poly(St–MMA–AA) microspheres before total evaporation of the ink droplets. To overcome this challenge, on the one hand, hydrophobic PDMS surfaces were used as substrates to facilitate sliding of the three phase contact lines; on the other hand, ethylene glycol was added into the ink to slow down its evaporation. It was noteworthy that poly(St–MMA–AA) microspheres with suitable diameter should be selected to assemble into PCs with given photonic bandgap for the aim of enhancing QD's fluorescence emission.^[32] Here, poly(St–MMA–AA) microspheres with diameter of 281 nm were used, which assembled into PCs with photonic bandgap just overlapped the emission of the in situ fabricated QDs. The as-fabricated PC domes

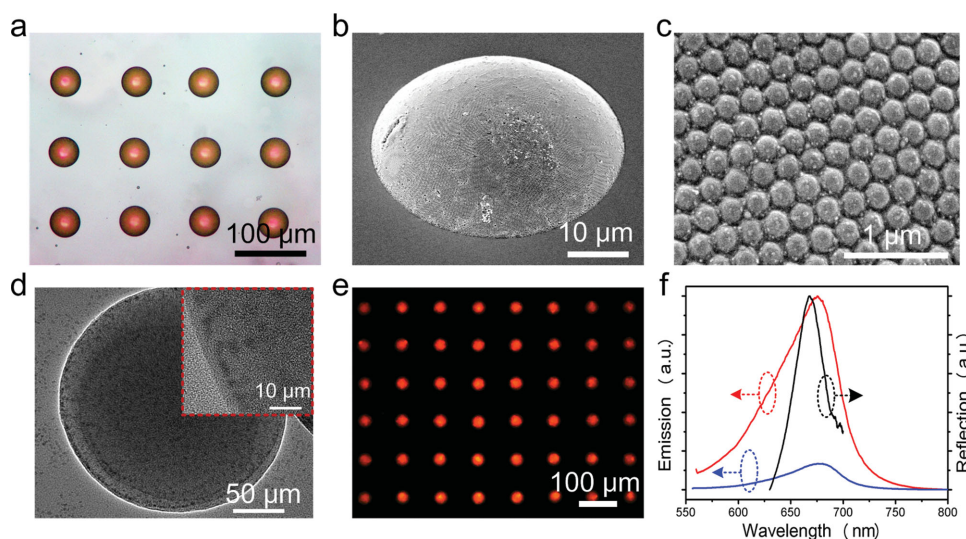


Figure 3. Fluorescent CdS QD-PC nanocomposite patterns are in situ fabricated by reactive inkjet printing and microsphere assembling. a) Optical microscope photograph of the CdS QD-PC nanocomposite dome array printed on PDMS substrate. b) 45° SEM observation of a single dome constructed by the nanocomposites. c) Magnified SEM image of the nanocomposites, revealing photonic crystal structures constructed by closely packed poly(St-MMA-AA) microspheres and randomly distributed CdS QDs. d) TEM observation of a single poly(St-MMA-AA) microsphere loaded with CdS QDs by in situ gas treatment. Insert is a high resolution image of the nanocomposites. e) Fluorescent image of the printed CdS QD-PC nanocomposite dome array. f) Reflection and emission spectra of the nanocomposite patterns, indicating the fluorescence enhancement of the QDs by the bandgap-matched photonic crystals. Red and blue lines represent the fluorescent emissions of CdS QDs-PCs nanocomposite before and after heat treatment, respectively.

were characterized by optical microscope and SEM, as shown in Figure S2 (Supporting Information). Optical microscope photograph of the PC dome array revealed the structural color of the PC domes (Figure S2a, Supporting Information). In a single PC dome, poly(St-MMA-AA) microspheres were closely packed, as demonstrated by the SEM observations in Figure S2 (b–d) (Supporting Information). Therefore, the added divalent cadmium ions in the PC ink had no effect on the assembly of the poly(St-MMA-AA) microspheres and PC domes were successfully fabricated by inkjet printing.

Fluorescent CdS QD-PC nanocomposite patterns were achieved by simply treating the cadmium source-loaded PC domes with hydrogen sulfide gas.^[8,33] **Figure 3** thoroughly demonstrates the morphological structures and optical properties of the CdS QD-PC nanocomposites. Figure 3a reveals that the color of the CdS QD-PC nanocomposite arrays became brown, which is a mixture of the red structural color of the PCs and the yellowish color of the in situ generated CdS QDs. In Figure 3b, 45° SEM observation of a single printed dot shows the dome structure with rare defects, indicating that the assembled PC structures were not damaged after gas treatment. A magnified SEM image of the nanocomposites in Figure 3c reveals the PC structures assembled by closely packed poly(St-MMA-AA) microspheres with randomly distributed CdS QDs. To further confirm the in situ generation of CdS QDs, TEM observations were carried out. The dilute PC ink was applied onto copper mesh-supported carbon films and dried in air, followed by hydrogen sulfide gas treatment. The TEM image of a single poly(St-MMA-AA) microsphere loaded with CdS QDs is given out in Figure 3d, coupled with a high resolution TEM image of the nanocomposites in the insert, where the dark dots clearly verify the generation of CdS QDs. Fluorescent image of the printed CdS

QD-PC nanocomposite dome array is shown in Figure 3e, demonstrating that bright orange red fluorescence is emitted by the nanocomposites. The photonic bandgap of the PC was centered at 668 nm, which overlapped with the emission of the QDs, as plotted by the black line in Figure 3f. The fluorescence enhancement of the QDs was investigated by comparing the emission intensities with and without the PC structures. Compared with samples treated by heating which destructed the periodic PC structures, the emission of the CdS QD-PC nanocomposites was highly enhanced, attributing to the efficient reflection of the bandgap-matched PC surface.

Fluorescent QD-contained nanocomposite patterns were of significance in high-efficiency luminescent devices, anti-counterfeiting technology and other related applications.^[34] To demonstrate the versatile patterning capability of reactive inkjet printing, dot-matrix-constructed fluorescent CdS QD-PC nanocomposite patterns were fabricated, as shown in **Figure 4**. Photograph and fluorescent image of a dot-matrix-constructed text pattern are shown in Figure 4a,b, respectively, indicative of the flexibility of the reactive inkjet printing technique. Meanwhile, a dot-matrix-constructed 2D code pattern was fabricated (Figure 4c), which would find numerous applications in encoding and anticounterfeiting. The detailed view of the dot matrix clearly revealed the regularly arranged pixels, manifesting the reliability of this method.

In conclusion, fluorescent CdS QD-PAA nanocomposite patterns were fabricated by reactive inkjet printing, and their fluorescence were enhanced by introducing monodispersed poly(St-MMA-AA) microspheres into the inks. Structural characterizations and optical measurements verified that monodispersed CdS QDs were generated after simple gas treatment of the printed patterns. Dot-matrix-constructed fluorescent CdS QD-PC nanocomposite patterns were printed

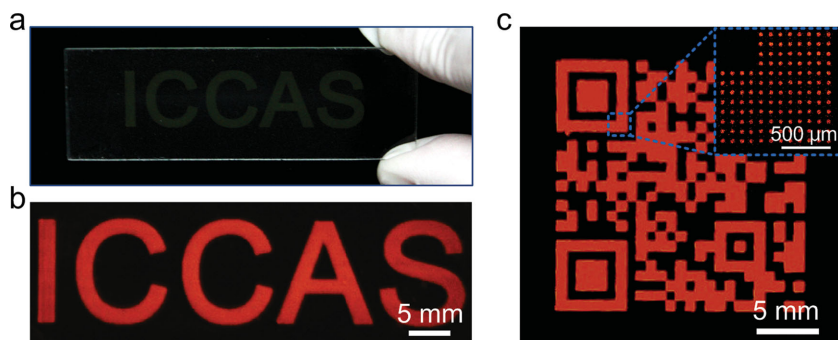


Figure 4. Dot-matrix-constructed fluorescent CdS QD-PC nanocomposite patterns are fabricated by reactive inkjet printing. a,b) Photograph and fluorescent image of a dot-matrix-constructed text pattern. c) Fluorescent image of a dot-matrix-constructed 2D code pattern. Inset is a detailed view of the dot matrix.

to demonstrate the versatile patterning capability of the reactive inkjet printing. This technique is flexible and efficient for controllable patterning of the QD-contained nanocomposites, and would be broadened to the fabrication of other functional nanomaterials and optoelectronic devices.

Experimental Section

Materials: PDMS (Sylgard 184) was purchased from Dow-Corning. PAA (with average molecule weight of 1800), cadmium chloride ($\text{CdCl}_2 \cdot 2.5\text{H}_2\text{O}$), and sodium sulfide ($\text{Na}_2\text{S} \cdot 9\text{H}_2\text{O}$) were purchased from Sigma-Aldrich and used as received. Hydrochloric acid, ethylene glycol, and ethanol were purchased from Sinopharm Chemical Reagent Co., Ltd and used as received. The monodispersed poly(St-MMA-AA) microspheres were synthesized by emulsion polymerization method.^[30] Deionized water was generated by Mini-Q water purification system.

Preparation of PDMS Substrates: PDMS base was mixed with a curing agent in the proportion of 10:1 by weight. The PDMS precursor was put into a centrifuge to remove air bubbles (5000 rpm, 5 min). Then the precursor was spin-coated onto commercially available PET or glass surfaces (firstly 800 rpm for 10 s, then 3000 rpm for 30 s). The PDMS precursor-coated surfaces were heated at 70 °C for 3 h to completely solidify the precursor.

Fabrication of CdS QD-PAA Nanocomposites: PAA (16 wt%) coupled with $\text{CdCl}_2 \cdot 2.5\text{H}_2\text{O}$ (0.2 M) were dissolved in water/ethanol mixed solvent (with volume ratio as 70:30) and used as the NC ink. The printing of the NC ink was performed by a Dimatix Fujifilm DMP-2831 printed with 10 pL Dimatix materials cartridge, which was controlled with the Dimatix Drop Manager software. Only one nozzle was used during the printing. The printing frequency was set at 3.0 kHz and a customized waveform was utilized. The printed patterns were dried in air and subsequently put into a glass container where hydrogen sulfide was generated by the reaction between sodium sulfide and dilute hydrochloric acid. After gas treatment for 1 h, the patterns were taken out and CdS QD-PAA nanocomposites were fabricated.

Fabrication of CdS QD-PC Nanocomposites: The PC inks were prepared by dispersing the poly(St-MMA-AA) microspheres (with latex concentration of 15 wt%) into a mixing solvent of deionized water (70 wt%) and ethylene glycol (30 wt%). Meanwhile, 0.2 M

$\text{CdCl}_2 \cdot 2.5\text{H}_2\text{O}$ was added into the ink to introduce cadmium source. The printing and gas treatment processes were the same as that in the fabrication of CdS QD-PAA nanocomposites.

Instruments and Characterization: The structures and morphologies of the CdS QD-PAA and CdS QD-PC nanocomposites were investigated by an optical microscope (Olympus MX40, Japan), a field-emission scanning electron microscope (JSM-7500, Japan), and a transmission electron microscope (JEM-2100F, Japan). The fluorescent images of the nanocomposites were obtained on a laser confocal microscope (Olympus FV1000-IX81, Japan). The large-scaled fluorescent images were taken by a fluorescence scanner (Champ-Chemi Professional+, China) with 365-nm UV light excitation. The UV-vis absorbance spectrum was obtained by an ultraviolet-visible spectrophotometer (UV-2600, Japan). The fluorescence spectrum was measured by a spectrometer (Princeton Instruments Acton SP2300, USA) equipped with a CCD camera (Princeton Instruments Pixis100, USA). The microreflectance spectrum observation of the PC was carried out by combining a reflected microscope (Olympus MX40, Japan) and a fiber optic UV-vis spectrometer (Ocean Optic HR 4000, USA). The illuminating light was focused onto the PC through an objective lens and the reflected light was collected by the same lens and then transported to the spectrometer through the optic fiber. The contact angles of the printing substrates were measured using a contact angle system (Dataphysics OCA20, Germany) at ambient temperature.

Supporting Information

Supporting Information is available from the Wiley Online Library or from the author.

Acknowledgements

The authors thank the continuous financial support of 973 Program (Nos. 2013CB933004, 2011CB932303 and 2011CB808400), the National Nature Science Foundation (Grant Nos. 51473173, 51173190, and 21121001), and the "Strategic Priority Research Program" of the Chinese Academy of Sciences (Grant No. XDA09020000). Dr. Linfeng Chen and Miss Wei Ran from the Institute of Chemistry, Beijing and Dr. Jianxin Kang from Beihang University are acknowledged for their helpful discussions and technical support.

- [1] a) A. P. Alivisatos, *Science* **1996**, 271, 933; b) X. Q. Li, Y. W. Wu, D. Steel, D. Gammon, T. H. Stievater, D. S. Katzer, D. Park, C. Piermarocchi, L. J. Sham, *Science* **2003**, 301, 809;

- c) D. Vanmaekelbergh, P. Liljeroth, *Chem. Soc. Rev.* **2005**, *34*, 299; d) J. Y. Kim, O. Voznyy, D. Zhitomirsky, E. H. Sargent, *Adv. Mater.* **2013**, *25*, 4986.
- [2] S. K. Panda, S. G. Hickey, H. V. Demir, A. Eychmüller, *Angew. Chem., Int. Ed.* **2011**, *50*, 4432.
- [3] a) Y. Shirasaki, G. J. Supran, M. G. Bawendi, V. Bulovic, *Nat. Photonics* **2013**, *7*, 13; b) X. Y. Yang, E. Mutlugun, Y. B. Zhao, Y. Gao, K. S. Leck, Y. Y. Ma, L. Ke, S. T. Tan, H. V. Demir, X. W. Sun, *Small* **2014**, *10*, 247.
- [4] a) A. J. Nozik, M. C. Beard, J. M. Luther, M. Law, R. J. Ellingson, J. C. Johnson, *Chem. Rev.* **2010**, *110*, 6873; b) Z. X. Pan, I. Mora-Sero, Q. Shen, H. Zhang, Y. Li, K. Zhao, J. Wang, X. H. Zhong, J. Bisquert, *J. Am. Chem. Soc.* **2014**, *136*, 9203.
- [5] a) K. Galatsis, K. L. Wang, M. Ozkan, C. S. Ozkan, Y. Huang, J. P. Chang, H. G. Monbouquette, Y. Chen, P. Nealey, Y. Botros, *Adv. Mater.* **2010**, *22*, 769; b) H. B. Lan, Y. C. Ding, *Nano Today* **2012**, *7*, 94.
- [6] W. W. Yu, X. G. Peng, *Angew. Chem Int. Ed.* **2002**, *41*, 2368.
- [7] a) D. Fragouli, V. Resta, P. P. Pompa, A. M. Laera, G. Caputo, L. Tapfer, R. Cingolani, A. Athanassiou, *Nanotechnology* **2009**, *20*, 9; b) F. Di Benedetto, A. Camposo, L. Persano, A. M. Laera, E. Piscopiello, R. Cingolani, L. Tapfer, D. Pisignano, *Nanoscale* **2011**, *3*, 4234.
- [8] Z. B. Sun, X. Z. Dong, W. Q. Chen, S. Nakanishi, X. M. Duan, S. Kawata, *Adv. Mater.* **2008**, *20*, 914.
- [9] L. L. Xu, C. F. Wang, S. Chen, *Angew. Chem Int. Ed.* **2014**, *53*, 3988.
- [10] a) A. Chiolerio, A. Virga, P. Pandolfi, P. Martino, P. Rivolo, F. Geobaldo, F. Giorgis, *Nanoscale Res. Lett.* **2012**, *7*, 502; b) C. Novara, F. Petracca, A. Virga, P. Rivolo, S. Ferrero, A. Chiolerio, F. Geobaldo, S. Porro, F. Giorgis, *Nanoscale Res. Lett.* **2014**, *9*, 527.
- [11] a) Y. Wang, Z. Y. Tang, M. A. Correa-Duarte, L. M. Liz-Marzan, N. A. Kotov, *J. Am. Chem. Soc.* **2003**, *125*, 2830; b) S. Jun, E. J. Jang, J. Park, J. Kim, *Langmuir* **2006**, *22*, 2407; c) C. Paquet, E. Kumacheva, *Adv. Funct. Mater.* **2007**, *17*, 3105; d) J. J. Park, P. Prabhakaran, K. K. Yang, Y. Lee, J. Lee, K. Lee, J. Hur, J. M. Kim, N. Cho, Y. Son, D. Y. Yang, K. S. Lee, *Nano Lett.* **2010**, *10*, 2310.
- [12] a) X. C. Wu, A. M. Bittner, K. Kern, *Adv. Mater.* **2004**, *16*, 413; b) J. J. Gassensmith, P. M. Erne, W. F. Paxton, M. Frascioni, M. D. Donakowski, J. F. Stoddart, *Adv. Mater.* **2013**, *25*, 223.
- [13] a) Y. S. Oh, K. H. Lee, H. Kim, D. Y. Jeon, S. H. Ko, C. P. Grigoropoulos, H. J. Sung, *J. Phys. Chem. C* **2012**, *116*, 11728; b) X. Yu, J. T. Pham, C. Subramani, B. Creran, Y. C. Yeh, K. Du, D. Patra, O. R. Miranda, A. J. Crosby, V. M. Rotello, *Adv. Mater.* **2012**, *24*, 6330.
- [14] a) V. Wood, M. J. Panzer, J. L. Chen, M. S. Bradley, J. E. Halpert, M. C. Bawendi, V. Bulovic, *Adv. Mater.* **2009**, *21*, 2151; b) E. Tekin, P. J. Smith, S. Hoepfner, A. M. J. van den Berg, A. S. Susha, A. L. Rogach, J. Feldmann, U. S. Schubert, *Adv. Funct. Mater.* **2007**, *17*, 23; c) J. Y. Kim, C. Ingrosso, V. Fakhfour, M. Striccoli, A. Agostiano, M. L. Curri, J. Brugger, *Small* **2009**, *5*, 1051; d) H. M. Haverinen, R. A. Myllylä, G. E. Jabbour, *Appl. Phys. Lett.* **2009**, *94*, 3.
- [15] a) P. J. Smith, A. Morrin, *J. Mater. Chem.* **2012**, *22*, 10965; b) T. Akagi, T. Fujiwara, M. Akashi, *Angew. Chem Int. Ed.* **2012**, *51*, 5493; c) P. Krober, J. T. Delaney, J. Perelaer, U. S. Schubert, *J. Mater. Chem.* **2009**, *19*, 5234; d) R. Zhang, A. Liberski, F. Khan, J. J. Diaz-Mochon, M. Bradley, *Chem. Commun.* **2008**, 1317; e) K. Kim, S. I. Ahn, K. C. Choi, *Carbon* **2014**, *66*, 172; f) D. P. Li, D. Sutton, A. Burgess, D. Graham, P. D. Calvert, *J. Mater. Chem.* **2009**, *19*, 3719.
- [16] M. Abulikemu, E. H. Da'as, H. Haverinen, D. Cha, M. A. Malik, G. E. Jabbour, *Angew. Chem Int. Ed.* **2014**, *53*, 420.
- [17] S. B. Walker, J. A. Lewis, *J. Am. Chem. Soc.* **2012**, *134*, 1419.
- [18] J. L. Zhuang, D. Ar, X. J. Yu, J. X. Liu, A. Terfort, *Adv. Mater.* **2013**, *25*, 4631.
- [19] a) K. Rajeshwar, N. R. de Tacconi, C. R. Chenthamarakshan, *Chem. Mater.* **2001**, *13*, 2765; b) A. Camposo, M. Polo, A. A. R. Neves, D. Fragouli, L. Persano, S. Molle, A. M. Laera, E. Piscopiello, V. Resta, A. Athanassiou, R. Cingolani, L. Tapfer, D. Pisignano, *J. Mater. Chem.* **2012**, *22*, 9787.
- [20] a) S. J. Byrne, Y. Williams, A. Davies, S. A. Corr, A. Rakovich, Y. K. Gun'ko, Y. R. Rakovich, J. F. Donegan, Y. Volkov, *Small* **2007**, *3*, 1152; b) C. Meng, Y. Xiao, P. Wang, L. Zhang, Y. X. Liu, L. M. Tong, *Adv. Mater.* **2011**, *23*, 3770.
- [21] a) Z. B. Sun, X. Z. Dong, S. Nakanishi, W. Q. Chen, X. M. Duan, S. Kawata, *Appl. Phys. A-Mater. Sci. Process.* **2007**, *86*, 427; b) J. Han, H. L. Su, D. Zhang, J. J. Chen, Z. X. Chen, *J. Mater. Chem.* **2009**, *19*, 8741; c) Y. J. Zhao, X. W. Zhao, B. C. Tang, W. Y. Xu, J. Li, L. Hu, Z. Z. Gu, *Adv. Funct. Mater.* **2010**, *20*, 976.
- [22] M. Sangermano, L. Vescovo, N. Pepino, A. Chiolerio, P. Allia, P. Tiberto, M. Coisson, L. Suber, G. Marchegiani, *Macromol. Chem. Phys.* **2010**, *211*, 2530.
- [23] A. Chiolerio, I. Roppolo, M. Sangermano, *RSC Adv.* **2013**, *3*, 3446.
- [24] a) M. X. Kuang, J. X. Wang, B. Bao, F. Y. Li, L. B. Wang, L. Jiang, Y. L. Song, *Adv. Opt. Mater.* **2014**, *2*, 34; b) M. X. Kuang, L. B. Wang, Y. L. Song, *Adv. Mater.* **2014**, *26*, 6950; c) M. X. Kuang, J. X. Wang, L. B. Wang, Y. L. Song, *Acta Chim. Sinica* **2012**, *70*, 1889.
- [25] B. J. de Gans, U. S. Schubert, *Langmuir* **2004**, *20*, 7789.
- [26] a) M. Singh, H. M. Haverinen, P. Dhagat, G. E. Jabbour, *Adv. Mater.* **2010**, *22*, 673; b) Z. L. Zhang, X. Y. Zhang, Z. Q. Xin, M. M. Deng, Y. Q. Wen, Y. L. Song, *Adv. Mater.* **2013**, *25*, 6714.
- [27] F. Villani, P. Vacca, G. Nenna, O. Valentino, G. Burrasca, T. Fasolino, C. Minarini, D. della Sala, *J. Phys. Chem. C* **2009**, *113*, 13398.
- [28] a) M. Moffitt, A. Eisenberg, *Chem. Mater.* **1995**, *7*, 1178; b) M. Moffitt, L. McMahon, V. Pessel, A. Eisenberg, *Chem. Mater.* **1995**, *7*, 1185.
- [29] a) S. P. Ogawa, M. Imada, S. Yoshimoto, M. Okano, S. Noda, *Science* **2004**, *305*, 227; b) M. Fujita, S. Takahashi, Y. Tanaka, T. Asano, S. Noda, *Science* **2005**, *308*, 1296; c) A. Blanco, H. Miguez, F. Meseguer, C. Lopez, F. Lopez-Tejiera, J. Sanchez-Dehesa, *Appl. Phys. Lett.* **2001**, *78*, 3181; d) F. Fleischhaker, R. Zentel, *Chem. Mater.* **2005**, *17*, 1346.
- [30] H. Li, J. X. Wang, H. Lin, L. Xu, W. Xu, R. M. Wang, Y. L. Song, D. B. Zhu, *Adv. Mater.* **2010**, *22*, 1237.
- [31] a) J. Hou, H. C. Zhang, Q. Yang, M. Z. Li, Y. L. Song, L. Jiang, *Angew. Chem Int. Ed.* **2014**, *53*, 5791; b) M. Z. Li, F. He, Q. Liao, J. Liu, L. Xu, L. Jiang, Y. L. Song, S. Wang, D. B. Zhu, *Angew. Chem Int. Ed.* **2008**, *47*, 7259; c) H. Li, J. X. Wang, Z. L. Pan, L. Y. Cui, L. A. Xu, R. M. Wang, Y. L. Song, L. Jiang, *J. Mater. Chem.* **2011**, *21*, 1730.
- [32] a) N. Ganesh, W. Zhang, P. C. Mathias, E. Chow, J. Soares, V. Malyarchuk, A. D. Smith, B. T. Cunningham, *Nat. Nanotechnol.* **2007**, *2*, 515; b) Y. Q. Zhang, J. X. Wang, Z. Y. Ji, W. P. Hu, L. Jiang, Y. L. Song, D. B. Zhu, *J. Mater. Chem.* **2007**, *17*, 90.
- [33] G. Majumdar, S. K. Gogoi, A. Paul, A. Chattopadhyay, *Langmuir* **2006**, *22*, 3439.
- [34] a) L. L. Zhu, Y. J. Yin, C. F. Wang, S. Chen, *J. Mater. Chem. C* **2013**, *1*, 4925; b) J. Zhang, L. T. Ling, C. F. Wang, S. Chen, L. Chen, D. Y. Son, *J. Mater. Chem. C* **2014**, *2*, 3610.

Received: October 9, 2014
 Revised: November 14, 2014
 Published online: